Kinetics of OH Radical Reactions with Methane in the Temperature Range 295−660 K and with Dimethyl Ether and Methyl-*tert*-butyl Ether in the Temperature Range 295−618 K

Amélie Bonard, Véronique Daële, Jean-Louis Delfau, and Christian Vovelle*

Laboratoire de Combustion et Systèmes Réactifs, CNRS and Université d'Orléans, 1C, avenue de la recherche scientifique, 45071 Orleans Cedex 2, France

The pulse laser photolysis/laser induced fluorescence (PLP−LIF) technique has been used to measure the rate constants of the reactions of OH radicals with dimethyl ether and methyl-*tert*-butyl ether. OH radicals were produced by photolysis of H_2O_2 at $\lambda = 266$ nm. The photolysis cell was heated by a small electric furnaces in order to obtain information on the temperature dependency of the rate constants in the domain of 295−660 K. A preliminary study of the reaction of OH with methane was carried out to control the experimental setup. The Arrhenius expression obtained in the temperature range of 295−668 K, $k_{OH+CH_4} = (5.65 \pm 0.49) \times 10^{-21}T^{3.01} \exp[-(959 \pm 36)/T]$, is in very good agreement with previous determinations (bimolecular rate constant units: cm^3 molecule^{-1} s^{-1}; error limits $\pm 2\sigma$). For the reactions of OH with ethers, the Arrhenius expressions derived from our own results are $k_{OH+DME}(295−618 \text{ K}) = (3.02 \pm 0.10) \times 10^{-20}T^{2.85} \exp[(618 \pm 13)/T]$ and $k_{OH+MTBE}(297−616 \text{ K}) = (6.59 \pm 0.43) \times 10^{-19}T^{2.40} \exp([(499 \pm 22)/T]$. Combining these data with those from previous experimental studies allows us to derive Arrhenius expressions in larger temperature domains: $k_{OH+DME}(230−650 \text{ K}) = (4.59 \pm 0.21) \times 10^{-19}T^{2.46} \exp[(476 \pm 14)/T]$ and $k_{OH+MTBE}(230−750 \text{ K}) = (1.58 \pm 0.09) \times 10^{-20}T^{2.93} \exp([(716 \pm 18)/T]$.

Introduction

There is a growing use of oxygenated compounds, especially organic ethers, as fuel additives with beneficial effects such as an increase of the octane number and a reduction of carbon monoxide and particles emissions. However, these additives can also enhance the exhaust emission of volatile organic compounds (VOCs) such as formaldehyde.[1] A better understanding of the influence of oxygenated fuel additives requires accurate data on their consumption kinetics in automotive engines. Normal combustion in an engine occurs essentially at high temperature (between 1500 and 2000 K), and kinetic data should be determined in this range. However, data obtained in a lower temperature range (from ambient to 800 K) are also of interest because important processes such as knock take place in this temperature domain.

In this work, the rate constants for the reactions of OH radicals with dimethyl ether (DME) and methyl-*tert*-butyl ether (MTBE) have been measured in the temperature range 295−618 K. Measurements have been performed using the pulsed laser photolysis/laser induced fluorescence (PLP−LIF) technique, with a reaction cell heated electrically. OH radicals were produced by photolysis of H_2O_2. The production of OH by thermal decomposition of H_2O_2 could increase the background signal and reduce the accuracy of the OH fluorescence measurements. Specific measurements of the fluorescence signal in the absence of the photolysis light showed that OH production by thermal decomposition of H_2O_2 was completely negligible up to 570 K. A progressive increase in the signal was observed at higher temperatures, but the photolysis remains the dominant process for the formation of OH up to 670 K.

* To whom correspondence should be addressed. Phone: 33 2 38 25 54 82. Fax: 33 2 38 69 60 04. E-mail: vovel@cnrs-orleans.fr.

Concerning the thermal stability of the organic reagent, it is likely, from experimental and modeling studies on the oxidation of DME[2] and MTBE,[3] that thermal degradation is negligible at a temperature lower than 750 K. However, we considered that it would be useful to perform preliminary measurements on the reaction of OH radicals with methane, a reagent with a better thermal stability than ethers. Also, this reaction has been extensively studied in a large temperature domain[4] with a very good agreement between several independent determinations.

Experimental Section

Figure 1 displays the main features of the experimental setup. The reaction cell is made of quartz and is heated by independent electrical furnaces in order to maintain a flat temperature profile in the reaction zone. Temperature measurements along the reaction cell axis showed that in the range 318−618 K the temperature gradient is less than 1.0 K cm^{-1}. These measurements were performed with a type K thermocouple introduced from the bottom of the reaction cell.

Reactants flow through a three concentric tubes assembly. The central one is closed at its end and contains a chromel−alumel thermocouple for temperature control. The molecular reactant, diluted by helium, flows through the intermediate tube, and an H_2O_2/He mixture flows through the external tube. Gas flow rates are controlled by mass flow meters with an individual accuracy of 3%.

The fourth harmonic of a Nd:YAG (GCR-100, Quanta-Ray) laser is used for the production of OH radicals in the ground state ($X^2\pi$ ($v'' = 0$)) by photolysis of H_2O_2 at $\lambda = 266$ nm. The OH concentration is monitored by laser-induced fluorescence using a Nd:YAG pumped-frequency dye laser. OH excitation at $\lambda = 282$ nm corresponds to the $X^2\pi$ ($v'' = 0$) → $A^2\Sigma^+$ ($v' = 1$) transition. The dye laser operates with Rodamine 590

Kinetics of OH Radical Reactions

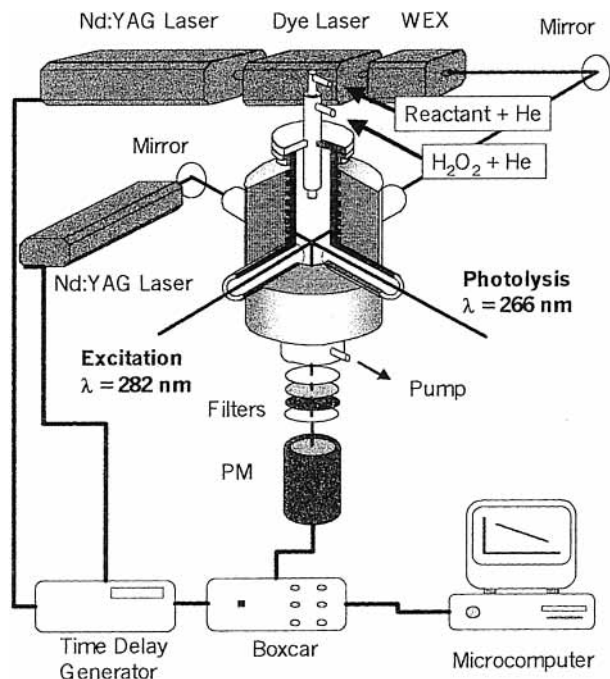*J. Phys. Chem. A, Vol. 106, No. 17, 2002* **4385**

Figure 1. Experimental setup.

in methanol. Both the photolysis and fluorescence lasers have repetition rates of 10 Hz. Typical pulse energies, measured at the exits of the reaction cell, are 10−45 mJ for the photolysis laser and slightly less than 1 mJ for the fluorescence laser. A time delay generator (Stanford Research System) synchronizes the laser shots at the preset reaction time.

A photomultiplier (PM) collects the radiation emitted in a direction perpendicular to the plane defined by the two laser beams. A filter with 310 nm peak transmission and 10 nm bandwidth selects the signals corresponding to the $A^2\Sigma^+$ ($v' = 0$) → $X^2\pi$ ($v'' = 0$) transition at $\lambda = 308$ nm and to the $A^2\Sigma^+$ ($v' = 1$) → $X^2\pi$ ($v'' = 1$) transition at $\lambda = 314$ nm. The output signal of the PM is integrated over a preset time period (gate width, 100 ns) by a Boxcar (EG&G, Princeton Applied Research) and transmitted to a microcomputer. The signal integration was repeated 128 times to increase the signal-to-noise ratio.

The reactant concentration is derived from its partial pressure in the reaction cell under the perfect gas assumption. To control that rate constant measurements are conducted under pseudo-first-order conditions, the OH radical concentration has been estimated from the H_2O_2 concentration with a quantum efficiency of 2^5 and an absorption cross section depending on the temperature.[6] The H_2O_2 concentration has been measured at room temperature by absorption of the 213.9 nm line from a zinc lamp. For these measurements, an absorption cell (1 m length) was connected to the exit of the reaction cell. A band-pass filter (214 nm peak transmission and 12 nm bandwidth) isolated the 213.9 nm line. The transmitted light was detected by a photodiode. All experiments on OH + DME and OH + MTBE reactions have been done with [organic reactant]/[OH] ratios above 100. This ratio is considerably higher ($>10^4$) for the reaction CH_4 + OH to make the secondary reaction CH_3 + OH negligible.

The certified purity of Helium (Alphagaz) was 99.9995%. Those of the reactants were 99.90% (methane, Alphagaz), 99% (DME, Fluka), and 99.8% (MTBE, Aldrich). Both ethers, liquid at ambient temperature, were purified by distillation prior to mixing with helium in a storage bottle. The initial H_2O_2/H_2O
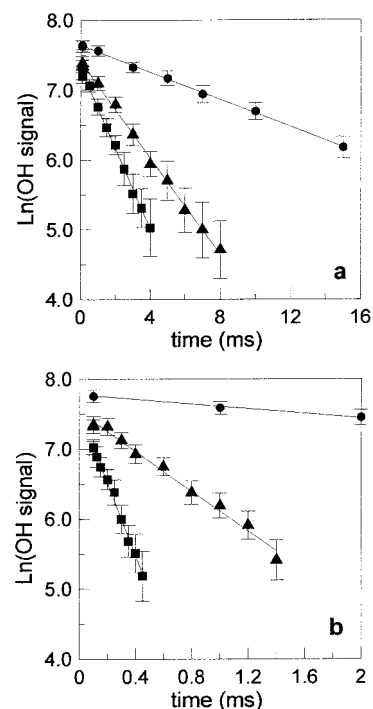

Figure 2. Reaction OH + CH_4. Evolution with time of the fluorescence signal. (a) $T = 295$ K; CH_4 concentration (molecule cm^{-3}), (●) 0.0; (▲) 4.05×10^{16}; (■) 6.95×10^{16}. (b) $T = 619$ K; CH_4 concentration (molecule cm^{-3}), (●) 0.0; (▲) 2.67×10^{15}; (■) 1.26×10^{16}.

(50/50%) solution was concentrated by bubbling of helium during 2 days.

Results and Discussion

(a) OH + CH_4 Reaction. The reaction of OH with methane has been studied in the temperature range of 295−668 K at a total pressure of 1.33×10^4 Pa (100 Torr). Figure 2 shows that the LIF signal (I_{OH}) decays exponentially in the whole domain of methane concentrations. The pseudo-first-order rate constants (k') were obtained by fitting the variations of $\ln(I_{OH})$ with time to straight lines by using a weighted linear least-squares procedure. As recommended by Cvetanovic et al.,[7] data were weighted by $w_i = 1/\sigma_i^2$ with $\sigma_i = \sigma_{I_{OH}}/I_{OH}$. $\sigma_{I_{OH}}$ is the mean standard deviation of the 128 OH fluorescence signal measurements. The value of k' obtained without methane was denoted k_0' and corresponds to the contribution of two terms: the consumption of OH by reaction with H_2O_2 ($k_{H_2O_2}[H_2O_2]$) and the diffusion of OH out of the detection zone (k_d). External consistency values were computed for the standard deviations of k' and k_0'.

Figure 3 shows the variation of the net pseudo-first-order rate ($k' - k_0'$) with the methane concentration. A linear relationship is observed for all temperatures studied, and rate constants of the bimolecular reaction of OH with CH_4 are derived from the slope of each straight line obtained from data fitting. Data were weighted by $w_i = 1/\sigma_i^2$ with $\sigma_i = [\sigma_k{}^2 + \sigma_{k_o'}{}^2]^{1/2}$. Table 1 lists the values and their error limits taken as twice the standard deviation. The range of OH and CH_4 concentrations are also mentioned in this table.

The Arrhenius plot of the rate constants measured in this work (Figure 4) exhibits a curvature, and a two step procedure was used to determine the three parameters of a modified Arrhenius expression: $k = AT^n \exp(-E/T)$. In the first step, variations of $\ln(k)$ with T were fitted to the expression $y = \ln(k) = \ln(A_1) +$

4386 *J. Phys. Chem. A, Vol. 106, No. 17, 2002*

Bonard et al.
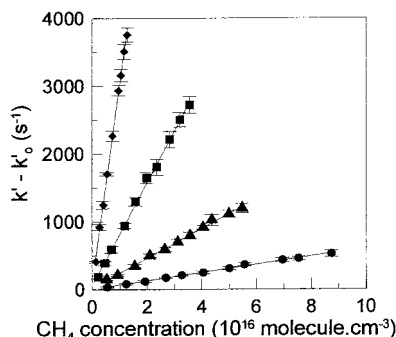
Figure 3. Reaction OH + CH$_4$. Evolution with the methane concentration of the net pseudo first-order rate constant. Temperature (K): (●) 295; (▲) 367; (■) 464; (◆) 619.
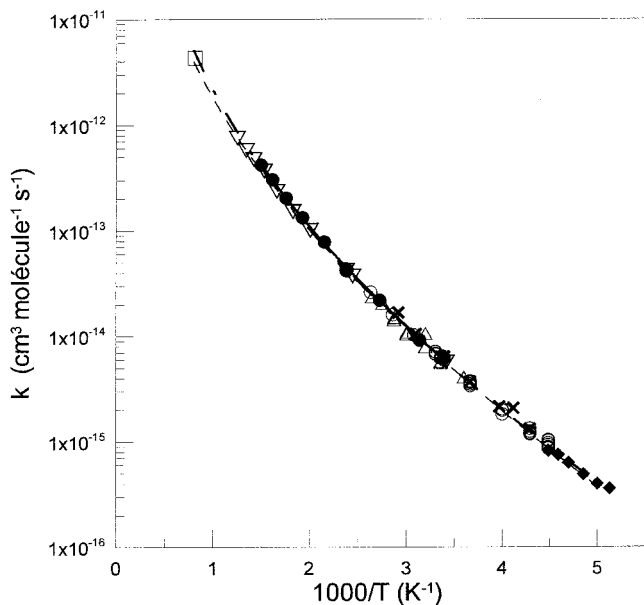
Figure 4. Reaction OH + CH$_4$. Arrhenius plot of the rate constant and comparison with previous experimental determinations. (●, this work; ×, Mellouki et al.;[12] ▽, Dunlop and Tully;[11] □, Bott and Cohen[8] ○, Vaghjiani and Ravishankara;[9] △, Finlayson-Pitts et al.;[10] ◆, Gierczak et al.;[13] modified Arrhenius equations: —, this work; − − −, Atkinson; - - -, all data.)

TABLE 1: Ranges of Reactant Concentrations and Reaction Rate Constants of the Reaction OH + CH$_4$ at a Total Pressure of 1.33×10^4 Pa (100 Torr)

temp (K)	range of OH concentration[a]	range of CH$_4$ concentration[b]	$k \pm 2\sigma$ (cm^3 molecule^{-1} s^{-1})
295	1.1−1.6	0.6−8.7	$(6.23 \pm 0.20) \times 10^{-15}$
319	1.2−1.2	0.5−8.2	$(9.16 \pm 0.28) \times 10^{-15}$
367	9.8−14.6	0.5−5.5	$(2.19 \pm 0.07) \times 10^{-14}$
419	2.1−2.7	0.4−4.0	$(4.26 \pm 0.18) \times 10^{-14}$
464	1.0−1.1	0.5−2.8	$(7.83 \pm 0.21) \times 10^{-14}$
519	2.5−4.7	0.2−2.6	$(1.33 \pm 0.04) \times 10^{-13}$
569	2.7−3.6	0.1−1.5	$(2.05 \pm 0.09) \times 10^{-13}$
619	6.4−7.0	0.1−1.5	$(3.06 \pm 0.10) \times 10^{-13}$
668	4.6−6.7	0.1−1.4	$(4.22 \pm 0.14) \times 10^{-13}$

^{a} 10^{11} molecule cm^{-3}. ^{b} 10^{16} molecule cm^{-3}.

$n_1 \ln(T) - E_1/T$ by a nonlinear least-squares procedure. Data were weighted by $w_i = 1/\sigma_{y_i}^2$ with $\sigma_{y_i} = \sigma_{k_i}/k_i$, and values of A_1, n_1, and E_1 were obtained from minimization of the sum $S = \sum_{i=1}^{N} w_i(y_i - \ln(A_1) - n_1\ln(T_i) + E_1/T_i)^2$. In the second step, A_2 and E_2 values and their errors σ_{A_2} and σ_{E_2} were computed from fitting of the data to the expression $z = \ln(k/T^{n_1}) = \ln(A_2) - E_2/T$. In this second step, a linear least-squares procedure was

used with data weighted by $w_i = 1/\sigma_{z_i}^2$ and $\sigma_{z_i} = \sigma_{k_i}/k_i$. The best fit so obtained corresponds to the expression

$$k_{OH+CH_4} \text{ (this work)} = (5.65 \pm 0.49) \times$$
$$10^{-21}T^{3.01} \exp[-(959 \pm 36)/T] \text{ cm}^3 \text{ molecule}^{-1} \text{ s}^{-1}$$

Kinetic data[8−12] previously measured with different techniques (shock tube, flow reactor, and photolysis cell) have been also plotted in Figure 4. Dunlop and Tully[11] determined the rate constant between 293 and 800 K. They mentioned an outstanding agreement between their values and those measured between 223 and 420 K by Vaghjiani and Ravishankara.[9] From both sets of data, they derive a modified Arrhenius expression:

$$k_{OH+CH_4} \text{ (Dunlop and Tully)} =$$
$$9.65 \times 10^{-20}T^{2.58} \exp(-1082/T) \text{ cm}^3 \text{ molecule}^{-1} \text{ s}^{-1}$$

Atkinson[4] observed that this expression is also in excellent agreement with the measurements performed by Bott and Cohen[8] at 1234 K, Finlayson-Pitts et al.[10] (278−378 K), and Mellouki et al.[12] (233−343 K) and proposed to extend the validity of the Dunlop and Tully expression to the temperature range 233−1234 K.

Our measurements are also in excellent agreement with all values considered by Atkinson, especially between 295 and 420 K, so that it can be assumed that error sources were minimized. The main error sources, secondary reaction of OH with CH$_3$ and reactions of OH with methane impurities such as alkenes, would both lead to an overestimation of the rate constant of the OH + CH$_4$ reaction. Because of the fast increase of the rate constant of the OH + CH$_4$ reaction with the temperature, this overestimation would be maximum at low temperature. In the temperature range 600−668 K, the three parameter expression obtained in this work predicts values 15% larger than those calculated by the Atkinson's expression. This slight difference can result from problems related to the thermal stability of H$_2$O$_2$. However, it may be also considered that only one data set[11] covers this temperature range in Atkinson's recommendation. When all data plotted in Figure 4, including very recent measurements performed by Gierczak et al.[13] with the PLP-LIF technique between 195 and 296 K, are taken into account, the following three parameter expression is obtained in the temperature range 195−1234 K:

$$k_{OH+CH_4} \text{ (all data of Figure 4)} = (4.09 \pm 0.18) \times$$
$$10^{-21}T^{3.04} \exp[-(920 \pm 13)/T] \text{ cm}^3 \text{ molecule}^{-1} \text{ s}^{-1}$$

The largest difference with respect to Atkinson's recommendation is only 5%.

(b) OH + CH$_3$OCH$_3$ Reaction. This reaction has been studied in the temperature range of 295−618 K at a total pressure of 1.33 10^4 Pa (100 Torr). As for the reaction with methane, exponential decays of the OH signal are observed over at least three lifetimes. Figure 5 shows the variation of the net pseudo-first-order reaction rate with the DME concentration, for three temperatures. Straight lines are obtained, and a weighted linear least-squares procedure is used to derive the rate constants of the OH + DME reaction. Values obtained and the ranges of OH and DME concentrations are listed in Table 2.

A partial decomposition of DME by the $\lambda = 266$ nm radiation of the photolysis laser is not expected to affect the accuracy of the results because DME does not absorb radiations with wavelengths above 200 nm.[14] However, the absence of photolysis

Kinetics of OH Radical Reactions

J. Phys. Chem. A, Vol. 106, No. 17, 2002 **4387**
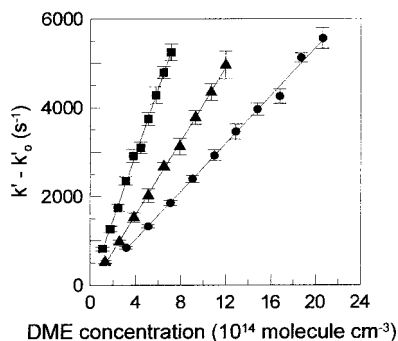
Figure 5. Reaction OH + DME. Evolution with the DME concentration of the net pseudo-first-order rate constant. Temperature (K): (●) 297; (▲) 433; (■) 618.

TABLE 2: Ranges of Reactant Concentrations and Reaction Rate Constants of the Reaction OH + DME at a Total Pressure of 1.33×10^4 Pa (100 Torr)

temp (K)	range of OH concentration[a]	range of DME concentration[b]	$k \pm 2\sigma$ (cm^3 molecule^{-1} s^{-1})
295[c]	0.5–0.6	3.2–18.7	$(2.70 \pm 0.08) \times 10^{-12}$
297	0.5	2.5–18.2	$(2.69 \pm 0.07) \times 10^{-12}$
298[d]	0.8–0.9	2.4–20.2	$(2.67 \pm 0.07) \times 10^{-12}$
317	0.7–0.8	2.7–18.1	$(2.85 \pm 0.06) \times 10^{-12}$
369	0.9–1.0	2.4–15.5	$(3.34 \pm 0.11) \times 10^{-12}$
433	1.0	1.3–12.0	$(4.07 \pm 0.11) \times 10^{-12}$
499	1.3	1.6–10.9	$(5.19 \pm 0.14) \times 10^{-12}$
567	2.4–2.6	1.2–7.7	$(6.21 \pm 0.12) \times 10^{-12}$
617[e]	2.7–2.8	1.1–7.1	$(7.54 \pm 0.20) \times 10^{-12}$
618	1.3–1.4	0.5–4.5	$(7.31 \pm 0.24) \times 10^{-12}$

[a] 10^{11} molecule cm^{-3}. [b] 10^{14} molecule cm^{-3}. [c] Pulse energy of the photolysis laser multiplied by a factor of 2. [d] Reactants flow velocity changed by a factor of 0.5. [e] Reactants flow velocity changed by a factor of 2.

of DME was verified by repeating one measurement at ambient temperature with the pulse energy of the photolysis laser increased by a factor of 2. The value so obtained, 2.70×10^{-12} cm^3 molecule^{-1} s^{-1}, is very close (within the incertitude range) to those obtained with the current laser pulse energy (2.69×10^{-12} cm^3 molecule^{-1} s^{-1}). A second control was made to test for a possible influence of the reactants jets velocity in the concentric tubes. Results obtained at ambient temperature and at 617 K show that the variations with respect to the values measured at the nominal velocities are within the incertitude ranges.

Values obtained in this work have been compared to previous experimental determinations of the rate constant of the OH + DME reaction performed using either relative[15,16] or absolute methods.[16–21] Most determinations cover a limited temperature domain (240–440 K), and only one (Arif et al.[21]) gives information on the temperature dependence of the rate constant in a larger temperature domain (295–650 K). Arif et al. observed that the extension of the temperature range at values higher than 440 K clearly shows a marked curvature in the Arrhenius plot. A nonlinear least-squares analysis leads to a modified Arrhenius expression:

$$k_{\text{OH+DME}} \text{ (Arif et al.)} = (3.39 \pm 13.8) \times$$
$$10^{-24} T^{(4.11 \pm 0.6)} \exp[(1221 \pm 252)/T] \text{ cm}^3 \text{ molecule}^{-1} \text{ s}^{-1}$$

Because $n = 4.11$ seems unreasonably high, Arif et al. proposed a second expression with n fixed at 2.0:

$$k_{\text{OH+DME}} \text{ (Arif et al.)} = (1.05 \pm 0.10) \times$$
$$10^{-17} T^{2.0} \exp[(328 \pm 32)/T] \text{ cm}^3 \text{ molecule}^{-1} \text{ s}^{-1}$$
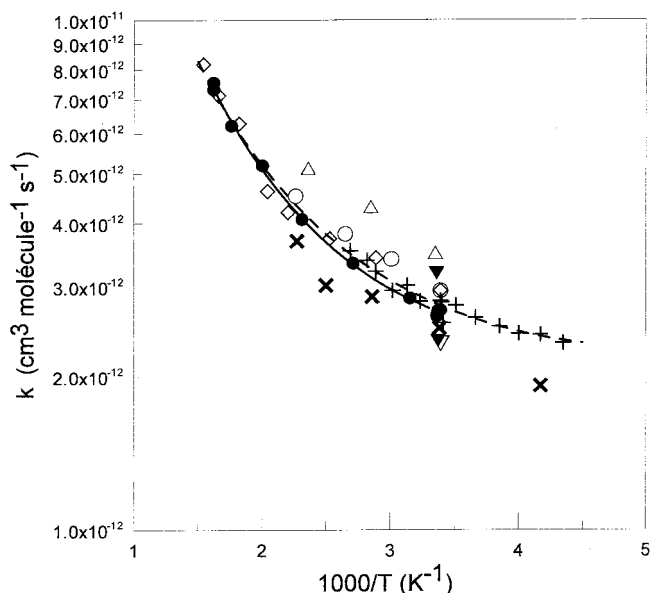
Figure 6. Reaction OH + DME. Arrhenius plot of the rate constant and comparison with previous experimental determinations. (●, this work; ×, Wallington et al.;[19] ▽, Wallington et al.;[15] ○, Tully and Droege;[18] △, Perry et al.;[17] +, Mellouki et al.;[20] ◇, Arif et al.;[21] ▼, Nelson et al.;[16] modified Arrhenius equations: —, this work; - - -, all data.)

The Arrhenius plot in Figure 6 includes all previous determinations and those from this work. Our values confirm the curvature of the Arrhenius plot but less pronounced than that from Arif et al.'s study. The two step procedure used for the OH + CH$_4$ reaction was applied to compute the parameters of a modified Arrhenius expression in the temperature range 295–618 K:

$$k_{\text{OH+DME}} \text{ (this work)} = (3.02 \pm 0.10) \times$$
$$10^{-20} T^{2.85} \exp[(618 \pm 13)/T] \text{ cm}^3 \text{ molecule}^{-1} \text{ s}^{-1}$$

Using the same fitting procedure, a second modified Arrhenius expression was derived from all values plotted in Figure 6. In the temperature range 230–650 K, this expression is

$$k_{\text{OH+DME}} \text{ (all data of Figure 6)} = (4.59 \pm 0.21) \times$$
$$10^{-19} T^{2.46} \exp[(476 \pm 14)/T] \text{ cm}^3 \text{ molecule}^{-1} \text{ s}^{-1}$$

However, marked variations in σ values are observed from one group to another. These variations result essentially from differences in the definition of σ which include sometimes experimental uncertainties in addition to statistical uncertainties. With data weighting by $w_i = 1/\sigma_i^2$, data with large σ values exert only a small influence on the parameters of the Arrhenius expression. Data fitting was also performed without weighting and the following expression was obtained:

$$k_{\text{OH+DME}} \text{ (all data of Figure 6)} = (1.17 \pm 0.11) \times$$
$$10^{-18} T^{2.33} \exp[(423 \pm 35)/T] \text{ cm}^3 \text{ molecule}^{-1} \text{ s}^{-1}$$

(c) OH + (CH$_3$)$_3$COCH$_3$ Reaction. If only one reaction path has to be considered for the reaction with DME, OH + CH$_3$OCH$_3$ = H$_2$O + CH$_3$OCH$_2$, the reaction with MTBE involves two paths: (A) OH + (CH$_3$)$_3$COCH$_3$ = H$_2$O + (CH$_3$)$_3$-COCH$_2$ and (B) OH + (CH$_3$)$_3$COCH$_3$ = H$_2$O + CH$_2$(CH$_3$)$_2$-COCH$_3$. Because the reaction products were not analyzed in this work, the measurements of the rate constant refer to the sum of the two reaction paths. These measurements have been

4388 *J. Phys. Chem. A, Vol. 106, No. 17, 2002*

Bonard et al.
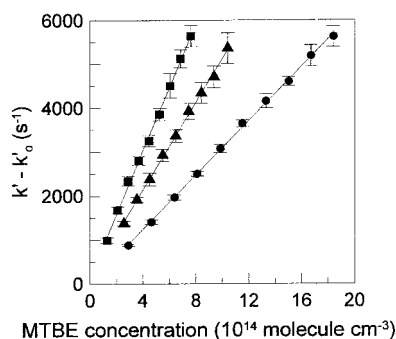
Figure 7. Reaction OH + MTBE. Evolution with the MTBE concentration of the net pseudo-first-order rate constant. Temperature (K): (●) 316; (▲) 498; (■) 616.

TABLE 3: Ranges of Reactant Concentrations and Reaction Rate Constants of the Reaction OH + MTBE at a Total Pressure of 1.33×10^4 Pa (100 Torr)

temp (K)	range of OH concentration	range of MTBE concentration	$k \pm 2\sigma$ (cm^3 molecule^{-1} s^{-1})
297	0.5–0.6	3.1–19.6	$(3.15 \pm 0.04) \times 10^{-12}$
297^c	0.7	2.5–19.8	$(3.01 \pm 0.09) \times 10^{-12}$
297^d	1.1–1.2	2.5–20.8	$(3.08 \pm 0.09) \times 10^{-12}$
298^e	0.2	1.2–9.66	$(2.96 \pm 0.04) \times 10^{-12}$
316	0.7–0.8	2.9–18.4	$(3.13 \pm 0.05) \times 10^{-12}$
367	0.9–1.0	2.5–16.0	$(3.71 \pm 0.07) \times 10^{-12}$
433	1.2–1.3	2.1–13.5	$(4.47 \pm 0.10) \times 10^{-12}$
498	1.7–2.0	1.6–10.4	$(5.26 \pm 0.18) \times 10^{-12}$
566	2.1–2.4	1.4–9.1	$(6.40 \pm 0.14) \times 10^{-12}$
616	3.6–3.7	1.3–8.4	$(7.27 \pm 0.27) \times 10^{-12}$
616^f	2.4–2.6	0.7–4.7	$(7.34 \pm 0.23) \times 10^{-12}$
616^e	0.8–0.9	0.6–4.3	$(7.42 \pm 0.22) \times 10^{-12}$

^{a} 10^{11} molecule cm^{-3}. ^{b} 10^{14} molecule cm^{-3}. ^{c} Pulse energy of the photolysis laser multiplied by a factor of 2. ^{d} Reactants flow velocity changed by a factor of 0.5. ^{e} Total pressure 6.65 kPa. ^{f} Reactants flow velocity changed by a factor of 2.

performed in the temperature range of 297–616 K, at a total pressure of 1.33×10^4 Pa (100 Torr). Here again, the exponential decay of the OH signal is observed over three lifetimes. Figure 7 shows that the net pseudo-first-order rate constant increases linearly with the MTBE concentration. For clarity purpose only, three temperature data have been plotted. At each temperature, the rate constant is calculated by a weighted linear least-squares analysis. Table 3 lists the values obtained in this way and the ranges of OH and MTBE concentrations.

The potential influence of either the pulse energy of the photolysis laser or of the reactants velocity has been also tested and found negligible as for DME. The effect of the total pressure has also been examined at ambient temperature and at 616 K. A reduction by a factor of 2 does not produce a significant change in the rate constant.

As for the reaction with DME, most determinations of the rate constant of the OH + MTBE reaction have been performed either at room temperature or in limited temperature domains.

Results obtained by using relative methods at room temperature, by different groups, have been compared in Table 4. These values are in reasonable agreement. Complementary kinetic studies have been carried out to derive information on the temperature dependency of the rate constant. Between 240 and 440 K, Wallington et al.[25] obtained a linear Arrhenius plot with a small positive temperature dependency of the rate constant. From a linear least-squares analysis, these authors derived a two parameters Arrhenius expression:

$$k_{OH+MTBE} \text{ (Wallington et al.)} = (5.1 \pm 1.6) \times$$
$$10^{-12} \exp[-(155 \pm 100)/T] \text{ cm}^3 \text{ molecule}^{-1} \text{ s}^{-1}$$

In the temperature range 246–314 K, Bennett and Kerr[26] also observed a small positive temperature dependency and derived from their own experimental results the following Arrhenius expression:

$$k_{OH+MTBE} \text{ (Bennett et al.)} = (4.0 \pm 1.3) \times$$
$$10^{-12} \exp[-(102 \pm 70)/T] \text{ cm}^3 \text{ molecule}^{-1} \text{ s}^{-1}$$

and

$$k_{OH+MTBE} \text{ (Bennett et al., evaluation)} = (5.2 \pm 1.7) \times$$
$$10^{-12} \exp[-(155 \pm 100)/T] \text{ cm}^3 \text{ molecule}^{-1} \text{ s}^{-1}$$

when data from others groups are also taken into account.

From measurements in the temperature range of 230–371 K, a slight curvature in the Arrhenius plot is mentioned by Téton et al.,[27] and a three parameter Arrhenius expression is proposed:

$$k_{OH+MTBE} \text{ (Téton et al.)} = (7.92 \pm 0.40) \times$$
$$10^{-17} T^2 \exp[(447 \pm 32)/T] \text{ cm}^3 \text{ molecule}^{-1} \text{ s}^{-1}$$

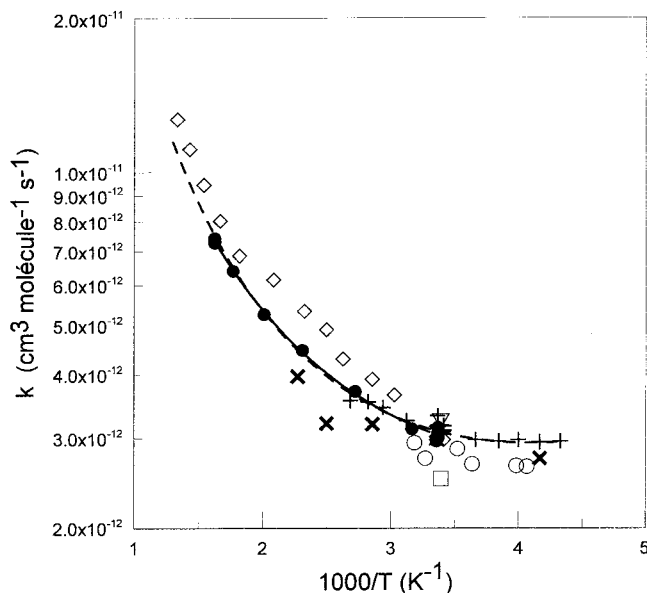However, for comparison purpose, these authors also propose an Arrhenius expression

$$k_{OH+MTBE} \text{ (Téton et al.)} = (5.03 \pm 0.27) \times$$
$$10^{-12} \exp[-(133 \pm 30)/T] \text{ cm}^3 \text{ molecule}^{-1} \text{ s}^{-1}$$

in very close agreement with Wallington's and Bennett's expressions.

Arif et al.[21] extended markedly the temperature domain toward higher values (293–750 K) and observed a marked curvature in the Arrhenius plot. From data fitting by a nonlinear least-squares procedure, these authors derive a three parameters expression:

$$k_{OH+MTBE} \text{ (Arif et al.)} = (1.11 \pm 3.18) \times$$
$$10^{-17} T^{(2.04 \pm 0.4)} \exp[(266 \pm 177)/T] \text{ cm}^3 \text{ molecule}^{-1} \text{ s}^{-1}$$

All data considered in this discussion and those obtained in this work have been plotted in Figure 8. From our own results,

TABLE 4: Comparison of Relative Determinations of the Rate Constant of the OH + MTBE Reaction at Ambient Temperature

T (K)	OH precursor	reference organics	k_{OH+Ref} (cm^3 molecule^{-1} s^{-1})	$k \pm 2\sigma$ (cm^3 molecule^{-1} s^{-1})	ref
295 ± 2	HONO	C_2H_4	8.0×10^{-12}	$(2.6 \pm 0.5) \times 10^{-12}$	22
295 ± 2	HONO	n-C_6H_{14}	5.9×10^{-12}	$(2.4 \pm 0.4) \times 10^{-12}$	22
298	CH_3ONO	n-C_4H_{10}	2.5×10^{-12}	$(3.24 \pm 0.08) \times 10^{-12}$	15
298	CH_3ONO or HONO	n-C_4H_{10}	2.54×10^{-12}	$(2.99 \pm 0.12) \times 10^{-12}$	23
298 ± 4	H_2O_2 or CH_3ONO	n-C_5H_{12}	3.96×10^{-12}	$(2.98 \pm 0.06) \times 10^{-12}$	24
298	$CH_3ONO + NO$	$C_2H_5OC_2H_5$	1.08×10^{-11}	$(2.84 \pm 0.08) \times 10^{-12}$	26
298	$CH_3ONO + NO$	$C_2H_5OC_2H_5$	1.29×10^{-11}	$(3.09 \pm 0.08) \times 10^{-12}$	26

Kinetics of OH Radical Reactions

J. Phys. Chem. A, Vol. 106, No. 17, 2002 **4389**

Figure 8. Reaction OH + MTBE. Arrhenius plot of the rate constant and comparison with previous experimental determinations. (●, this work; □, Cox and Goldstone;[22] ○, Bennett and Kerr;[26] ×, Wallington et al.;[25] ▽, Wallington et al.;[15] △, Smith et al.;[23] +, Téton et al.;[27] ◇, Arif et al.;[21] ◆, Picquet et al.;[24] modified Arrhenius equations: —, this work; - - -, all data.)

the two steps least-squares analysis leads to the following expression, in the temperature domain 297−616 K:

$$k_{OH+MTBE}\text{(this work)} = (6.59 \pm 0.43) \times$$
$$10^{-19}T^{2.40}\exp[(499 \pm 22)/T]\ cm^3\ molecule^{-1}\ s^{-1}$$

The solid line in Figure 8 corresponds to this expression. Considering all data reported on this figure, the two steps least-squares analysis with data weighting by $w_i = 1/\sigma_i^2$ leads to a second expression, in the temperature range of 230−750 K:

$$k_{OH+MTBE}\text{(all data of Figure 8)} = (1.58 \pm 0.09) \times$$
$$10^{-20}T^{2.93}\exp[(716 \pm 36)/T]\ cm^3\ molecule^{-1}\ s^{-1}$$

The same procedure applied without data weighting leads to

$$k_{OH+MTBE}\text{(all data of Figure 8)} = (3.97 \pm 0.25) \times$$
$$10^{-21}T^{3.15}\exp[(752 \pm 54)/T]\ cm^3\ molecule^{-1}\ s^{-1}$$

Conclusions

A heated PLP−LIF cell has been used to measure absolute rate constants for reactions of OH radicals with DME and MTBE in the temperature ranges 295−618 and 297−616 K, respectively. The maximum temperature can be limited by thermal degradation of either the H_2O_2 used as OH radicals precursor or the organic reagent. From specific measurements of the OH fluorescence signal in the absence of the photolysis light, it was shown that the first problem is negligible up to 570 K and not crucial up to 670 K. This point was also controlled by measuring the rate constant of the extensively studied reaction OH + CH_4. Values obtained are in good agreement with previous determinations, especially in the temperature range of 295−420 K

where several data sets are available. At higher temperatures, our measurements are slightly larger than those of Dunlop and Tully but differ from the Atkinson recommendation by less than 5%.

For the OH + DME reaction, this study confirms the curvature of the Arrhenius plot and provides new values in agreement with both the low temperature determinations of Mellouki et al.[20] and the measurements of Arif et al.[21] between 295 and 650 K.

Measurements performed in this work for the reaction OH + MTBE reaction are in excellent agreement with previous data measured between 295 and 371 K by Téton et al.[27] At higher temperatures, our values are slightly smaller than those previously measured by Arif et al.[21]

References and Notes

(1) Guibet, J. C. *Carburants et Moteurs*; Nouvelle Edition, Editions Technip: Paris, 1997.

(2) Curran, H. J.; Pitz, W. J.; Westbrook, C. K.; Dagaut, P.; Boettner, J. C.; Cathonnet, M. *Int. J. Chem. Kinet.* **1998**, *30*, 229.

(3) Glaude, P. A.; Battin-Leclerc, F.; Judenherc, B.; Warth, V.; Fournet, R.; Côme, G. M.; Scacchi, G. *Combust. Flame* **2000**, *121*, 345.

(4) Atkinson R. *J. Phys. Chem. Ref. Data* **1997**, *26* (2), 215.

(5) Vaghjiani, G. L.; Ravishankara, A. R. *J. Chem. Phys.* **1990**, *92*, (2), 996.

(6) De More, W. B.; Sander, S. P.; Golden, D.; Hampson, R. F.; Kurylo, M. J.; Howard, C. J.; Ravishankara, A. R.; Kolb, C. E.; Molina, C. J. *NASA JPL Pub.* **1997**, *97*, 4.

(7) Cvetanovic, R. J.; Singleton, D. L.; Paraskevopoulos, G. *J. Phys. Chem.* **1979**, *83* (1), 50.

(8) Bott, J. F.; Cohen, N. *Int. J. Chem. Kinet.* **1989**, *21*, 485.

(9) Vaghjiani, G. L.; Ravishankara, A. R. *Nature* **1991**, *350* (6317), 406.

(10) Finlayson-Pitts, B. J.; Ezell, M. J.; Jayaweera, T. M.; Berko, H. N.; Lai, C. C. *Geophys. Res. Lett.* **1992**, *19* (13), 1371.

(11) Dunlop, J. R.; Tully, F. P. *J. Phys. Chem.* **1993**, *97*, 11148.

(12) Mellouki, A.; Téton, S.; Laverdet, G.; Quilgars, A.; Le Bras, G. *J. Chim. Phys.* **1994**, *91*, 473.

(13) Gierczak, T.; Talukdar, R.; Herndon, S. C.; Vaghjiani, G. L.; Ravishankara, A. R. *J. Phys. Chem. A* **1997**, *101*, 3125.

(14) Calvert, J.; Pitts, J. N., Jr. *Photochemistry*; Wiley: New York, 1966.

(15) Wallington, T. J.; Andino, J. M.; Skewes, L. M.; Siegl, W. O.; Japar, S. M. *Int. J. Chem. Kinet.* **1989**, *21*, 993.

(16) Nelson, L.; Rattigan, O.; Neavyn, R.; Sidebottom, H.; Treacy, J.; Nielsen, O. J. *Int. J. Chem. Kinet.* **1990**, *22*, 1111.

(17) Perry, R. A.; Atkinson, R.; Pitts, J. N., Jr. *J. Chem. Phys.* **1977**, *67*, 611.

(18) Tully, F. P.; Droege A. T. *Int. J. Chem. Kinet.* **1987**, *19*, 251.

(19) Wallington, T. J.; Liu, R.; Dagaut, P.; Kurylo, M. J. *Int. J. Chem. Kinet.* **1988**, *20*, 41.

(20) Mellouki, A.; Téton, S.; Le Bras, G. *Int. J. Chem. Kinet.* **1995**, *27*, 791.

(21) Arif, M.; Dellinger, B.; Taylor, P. H. *J. Phys. Chem. A* **1997**, *101*, 2436.

(22) Cox, R. A.; Goldstone, A. *Proceedings of the Second European Symposium on the Physico-Chemical Behaviour of Atmospheric Pollutants*, D. Reidel Publishing Co.: Dordrecht, The Netherlands, 1981; p 112.

(23) Smith, D. F.; Kleindienst, T. E.; Hudgens, E. E.; McIver, C. D.; Bufalini, J. J. *Int. J. Chem. Kinet.* **1991**, *23*, 907.

(24) Picquet, B.; Heroux, S.; Chebbi, A.; Doussin, J. F.; Durand-Jolibois, R.; Monod, A.; Loirat, H.; Carlier, P. *Int. J. Chem. Kinet.* **1998**, *30*, 839.

(25) Wallington, T. J.; Dagaut, P.; Liu, R.; Kurylo, M. J. *Environ. Sci. Technol.* **1988**, *22*, 842.

(26) Bennett, P. J.; Kerr J. A. *J. Atmos. Chem.* **1990**, *10*, 27.

(27) Téton, S.; Mellouki, A.; Le Bras, G. *Int. J. Chem. Kinet.* **1996**, *28*, 291.